

# TEM thin foil preparation for ceramic composites with multilayered matrix

X. Bourrat\*, M. Alrivie, A. Michaux

*Laboratoire des Composites Thermostructuraux (LCTS), UMR 5801 CNRS-SEO-UB1, Université Bordeaux 1,  
3 Allée de la Boétie, F-33600 Pessac, France*

Received 8 December 2003; received in revised form 6 February 2004; accepted 13 February 2004

Available online 20 June 2004

## Abstract

A method for preparing thin foils for transmission electron microscopy (TEM) has been developed in the field of ceramic matrix composites (CMC). These composites belong to the last generation. They are developed for high temperature applications in oxidative environment (1350 °C). They possess a self-healing capability. Their design is based on a multilayered matrix. A refinement of the regular ion-milling technique was necessary to thin the samples and to proceed to a full observation of the inner matrix of the composite by TEM. In a regular CMC, the matrix is homogeneous and thereafter it has not to be fully inspected from the fiber to the surface. This sampling technique unable to thin the complete sequence of the different layers in the vicinity of large pores where the ion-milling technique is known to be very difficult. High resolution TEM as well as electron energy loss spectroscopy can be managed anywhere in the core sequence of the matrix.

© 2004 Published by Elsevier Ltd.

**Keywords:** Ceramic matrix composite; Sampling; Transmission electron microscopy; TEM sample preparation

## 1. Introduction

The preparation of TEM specimens of monolithic ceramic or even ceramic composite (CMC) as SiC/SiC for example, has become routine.<sup>1</sup> The new generation of CMCs is different because of its multilayered matrix.<sup>2</sup> The need to study every layer together with the different interfaces requires a lot of attempt by a routine technique. This is due to the fact that the material is mounted in epoxy which is much more easily sputtered in a regular ion-milling machine than the ceramic layers as B<sub>4</sub>C or SiC. An example of such a CMC can be seen in Fig. 1. It represents a slice in a mechanical test specimen, cut following the schematic of Fig. 2, then polished and observed by optical microscopy.

This composite is a 2.5D carbon-reinforced ceramic composite. It has a matrix designed both to reach high mechanical performances<sup>3</sup> and to protect the carbon fiber reinforcement against oxidation. Above the elastic limit, if microcracking occurs in the matrix this smart material reacts with mechanical fuses and undergoes a self-healing mechanism, whenever the oxidation takes place. This is

provided by the multilayered structure of the matrix, comprising glass forming materials. The concept is based on a succession of Si<sub>x</sub>B<sub>y</sub>C<sub>z</sub> layers. Fig. 1 shows the transverse bundles (regarding the loading direction) in cross section. Matrix sequence appears to be much more complete at the surface than in the center. The variations of the reflectance are due to a broad range of compositions and/or crystallinity.

TEM inspection has to have access to each layer and interface. This is quite easy at the surface of the composite by means of a cross section. In the core of the material the inspection of the infiltrated matrix can be completed only in the location close to the largest pores that survive in the materials. Transmission electron microscopy (TEM) sampling has to be discussed in term of which attributes are desirable:<sup>4</sup> first a specimen has to be thin but also representative and unchanged from the bulk state. In the case of ceramics, it is recommended to manage a preparation before the final thinning with ion-milling. It is also said that ion-milling fails systematically at the vicinity of large pores: an enlargement of the pore is indeed systematically observed, with thick edges in the materials. The electronic transparency is not obtained.

Focus ion beam technique could be tried, but is too localized to be successful in this case. In this paper we managed to use a regular ion-milling technique but after filling the

\* Corresponding author. Tel.: +33-5-56-84-47-40;  
fax: +33-5-56-84-12-25.

E-mail address: [Bourrat@lcts.u-bordeaux.fr](mailto:Bourrat@lcts.u-bordeaux.fr) (X. Bourrat).

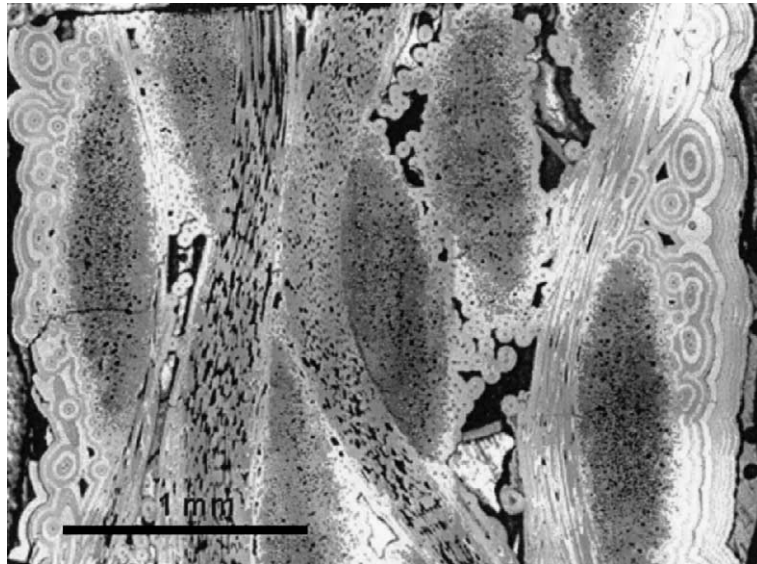


Fig. 1. Full section of the test specimen of the composite (slice of Fig. 2). The multilayered matrix can be easily seen in the outer zone (optical microscopy, natural light).

large porosity. Alumina cement is seen to be a good solution for that purpose.

## 2. Method of specimen preparation

This technique is applied on mechanical test specimen in order to expertise: (i) the chemical vapor infiltration (CVI) process performances, (ii) the failure micromechanics, or (iii) the oxidation resistance of the loaded sample at high temperature. For those purposes the specimen orientation is important: the zero degree bundles have to lie as longitudinal bundle in the TEM preparation. Sectioning and further operations are conducted following seven different steps.

### 2.1. Sectioning

Few thick slices are cut in the test specimen as shown in Fig. 2. These slices are 600–700  $\mu\text{m}$  thick and approximately 6 mm in length. The height is given by the thickness of the test specimen itself (2.5 mm in the example described in this paper). These thick slices are obtained by using a wire saw

(Escil, Switzerland) equipped with a 0.3 mm wire (60  $\mu\text{m}$  diamond). The lubricant has to be water-free (MM705 from Lamplan). The slices are cleaned with acetone.

### 2.2. Slice selection

The selection of the optimal section has to be conducted as follow. The optimum zone must be at the periphery of a 90° bundle (bundle in cross-section) surrounding a pore. The 90° bundle are preferably close to longitudinal bundles that strengthen the sample during the thinning. Such a situation can be seen on Fig. 3. This situation is not systematic, for that reason a few thick foils have to be cut. Most of the time the situation is optimum only on one side: the face of interest. Most of the mechanical thinning will be applied on the other one.

### 2.3. Mounting the material

At the outset, different operations of mounting and surfacing are necessary. The purpose is to impregnate the fine cracks with epoxy, to fill in the macroporosity with alumina and to realize a surfacing of both faces.

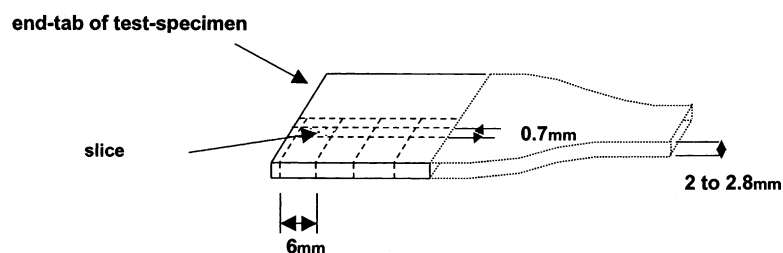


Fig. 2. Location of the sample in the mechanical test specimen (here in the end-tab). Note that the length of the slice is parallel to the tensile direction.

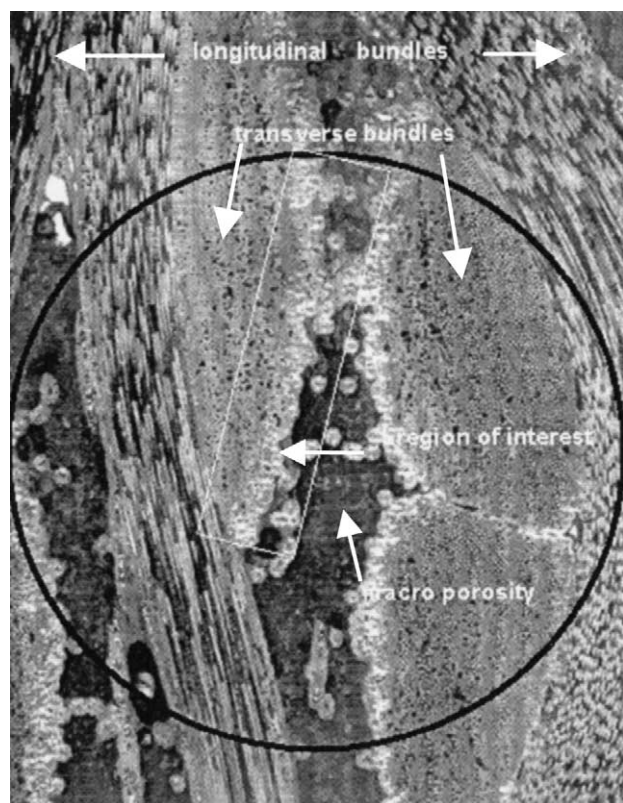


Fig. 3. Optical micrograph of a typical region of interest (the circle is 1 mm in diameter and corresponds to the TEM grid hole centered on the zone to be thinned) (same as Fig. 1, higher magnification).

The epoxy used is a gage adhesive with 70% of solvent (M-Bond 610 adhesive from Vishay). The as-sawn foils are placed in a small crystallizing dish and covered by a liberal amount of adhesive and placed in the embedding chamber at 50 kPa for 10 min at room temperature (Epovac impregnation apparatus from Struers). The foils are then put on a thick pad of silicone gum, dried 1 h and cured following the supplier indications (160 °C for 2 h in the case of M-Bond 610). This operation is repeated for three-times in the case of mechanical test specimen drawn to failure with of lot of cracks in it.

The second impregnation is managed to fill in the large pores. This is the additional step tested in this work, regarding the protocol used for a regular C/SiC material. An alumina cement was successfully tested and then used (reference 503 provided by AREMCO). This is a sub-micronic suspension of  $\text{Al}_2\text{O}_3$  in a polymer. The cement is forced inside the porosity, then dried and cured. For more details see Appendix A.

Next, both sides are straightened with a polishing machine using a 15  $\mu\text{m}$  (diamond plate) because the as-sawn surfaces are marked with grooves (Minimet from Buehler). In the example described in this paper, the starting thickness was 643  $\mu\text{m}$ , after the surfacing of the side of interest, it was 566  $\mu\text{m}$  and finally 417  $\mu\text{m}$  after the surfacing of the second one. It is important to minimize the grinding on the selected side.

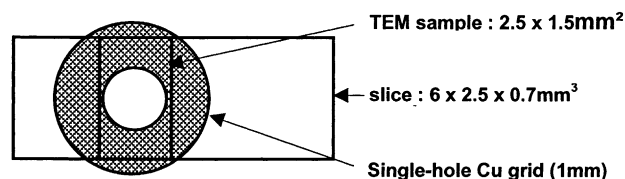


Fig. 4. Sampling for the TEM in the slice.

A second impregnation is conducted with the M-Bond 610 to close up all the residual porosity. This step was repeated for three-times with this material.

The final operation is a gentle surfacing of the opposite side with the polishing machine with the 30 and 15  $\mu\text{m}$  diamond plate to clean up the surface. The final thickness was then 415  $\mu\text{m}$ .

#### 2.4. Polishing of the face of interest

The purpose, now, is to realize the final polishing for preparing the ion-milling step on the face of interest. This polishing is preferably managed with the tripod polisher<sup>5,6</sup> for its gentle polishing (plane parallel polish). The slice is mounted on the Pyrex rod insert. For that purpose the L-shaped attachment is previously placed on the heater block itself on the 130 °C hot plate (slotted L-bracket, in this case). Some Quick Stick 135 wax (South Bay Technology) is put on the Pyrex rod surface. The slice is pressed on the melted wax. Any air bubble present is teased over. The slice is pressed with a back and forth motion to remove the wax excess. In order to realize a parallel polishing (with a wedge-polishing tripod) it is previously necessary to measure the initial thickness of the slice and the thickness once mounted on the Pyrex rod (slice + wax) with a micrometer (electronic micrometer Mitutoyo, Japan). The leveling is set (sample and two opposite micrometer feet) and then the 2 ft are simultaneously retracted with the value which is to grind away. The diamond lapping films successively used are: 30, 15, and 6  $\mu\text{m}$  (MDI from Escil) with the oil lubricant (L from Escil). A water-free lubricant is recommended with alumina cement. At each granulometry the thickness is measured: the starting value was 415  $\mu\text{m}$  and the final value 335  $\mu\text{m}$ . For more details see the abundant literature. The sample thickness is measured with an inverted high powered optical microscope (Reichert-Young MeF3) calibrated in  $\mu\text{m}$ .

After the polishing, the L-shaped attachment is left on the heater block (itself on the 130 °C hotplate) for a couple

Table 1  
Mechanical thinning and polishing with the tripod polisher

Film lapping polishing grit size ( $\mu\text{m}$ )	Polishing wheel speed control (rpm)	Final sample thickness ( $\mu\text{m}$ )
30	46.5	180
15	20–30	35
6	18–20	23
3	17	23



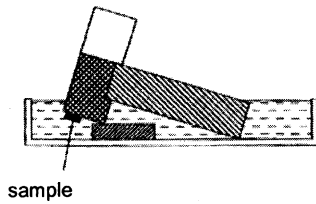


Fig. 5. Removal of a brittle sample from the L-shaped attachment of the tripod.

of minutes. Once the wax has become molten the sample is pushed to the edge of the rod so it can be picked off with tweezers. In the example of the present paper, the final value at the end was 335  $\mu\text{m}$ . The main mechanical thinning is not managed on this side.

#### 2.5. Drilling and sticking the specimen on the TEM copper grid

It is preferred to cut a small rectangular sample with the wire saw (in the slice) than drilling with an abrasive slurry

Table 2  
Conditions used for Ar-ion-milling

Angle ( $^{\circ}$ )	Tension (kV)	Intensity (mA)	Duration
20	7	1	1 h 35 min
15	7	1	30 min
13	7	1	10 min
12	7	1	45 min

disc cutter. First, the specimen is cut: 2.2 mm  $\times$  1.5 mm following the schematic diagram of Fig. 4. Then, before sticking the sample on the copper grid, both sample and grid are measured with the micrometer. TEM single-hole grids of 1 mm are used in this case. The face of interest is stuck on the grid with the M-Bond 610 adhesive, taking care to keep the targeted zone in the center. Drying and curing are managed following indications from supplier. Then the specimen and the grid thickness are measured with the micrometer (copper grid: 40  $\mu\text{m}$  and adhesive: 26  $\mu\text{m}$ ).

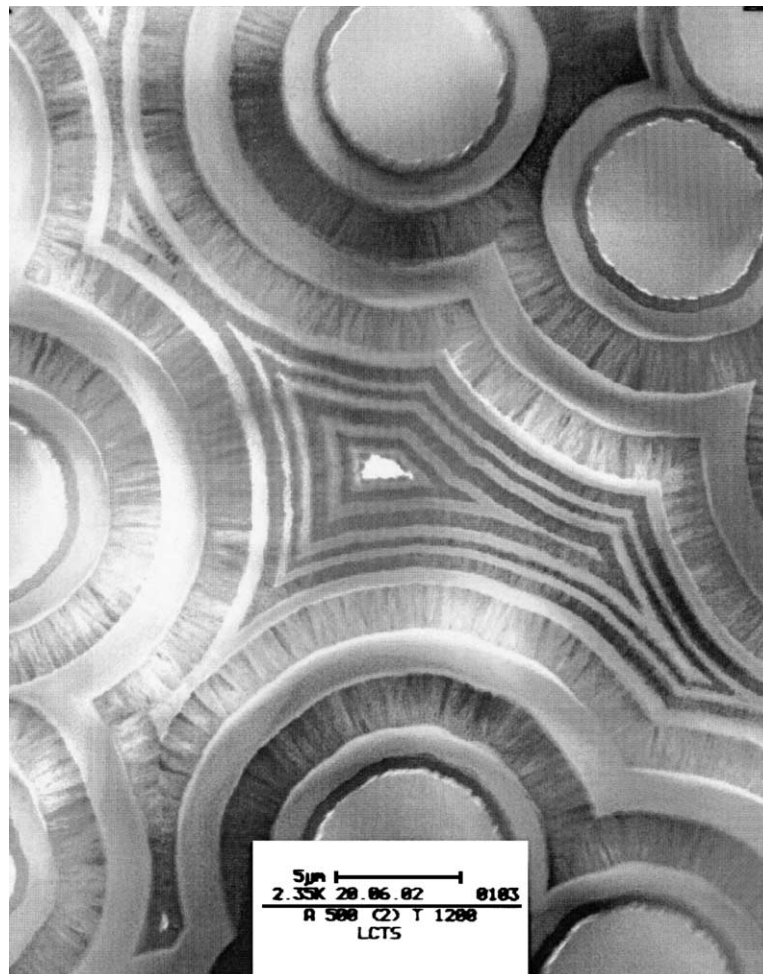


Fig. 6. Low magnification of a transverse bundle close to a macropore a complete series of matrix layers can be observed (TEM contrasted bright field, 2350 $\times$ ).

## 2.6. Mechanical thinning and polishing

As previously, the mechanical thinning is conducted with the tripod polisher. The specimen is mounted—copper down—onto the Pyrex rod insert. The thickness is controlled again (wax was 5  $\mu\text{m}$  in the example). Contrarily to the polishing of the first face (face of interest) a strong mechanical thinning is realized on the opposite face. Thus, the 30  $\mu\text{m}$  step is much longer. The progression used for the second face is given in Table 1. At the end, the final thickness obtained is 23  $\mu\text{m}$  (uncertainty on this measure is few  $\mu\text{m}$ ).

Removal of the sample is tricky. A large dish with a filter in the bottom is filled with acetone. The L-shaped attachment of the tripod is dismantled and put up-side-down in the dish on a glass slide (see Fig. 5). After 20 min the sample falls down on the filter. It is important to have previously mated the Pyrex rod surface to enhance the diffusion and make the wax more soluble (surfacing with the 15  $\mu\text{m}$ -grit film). Then the sample is dried on the filter (the sample needs to stay under the acetone level till it falls on the filter).

## 2.7. Ar-ion-milling

In this example a Duo Mill (ref: 600 from Gatan) was used at room temperature. The low temperature creates artifacts as fibers debonding for example. After cleaning, the sample is mounted in the holder with a sputter shield. The grid is stuck with three silver-paint contact points, copper-side down. Both guns are used with a continuous rotation. Conditions used in the example are reported on Table 2. The values are given in the case of a cathode in the first quarter of its lifetime. The optimal thinning is observed just after the disappearance of the transverse isolated fibers at the edge of macropores. Any way, an optical inspection is realized in transmission mode directly on the holder. At the electron transparency SiC is translucent,  $\text{Si}_x\text{B}_y\text{C}_z$  is orange-colored and pyrocarbon is no more impervious to light (brownish).

## 3. TEM examination

The requirement to meet with this material is the electron transparency of the complete matrix sequence in the core of the composite. Three kinds of parameters are needed: (i) the thickness of the layers and the “CVI/CVD ratio”, i.e. amount infiltrated in the core regarding that deposited at the surface, (ii) the structure of the layers and the nature of the interfaces. In this case high resolution is required and thus the thickness has to be of the same order as the mean free path for elastic scattering: lower than 50 nm (10 nm is an optimum if the amorphization is reduced<sup>7</sup>), (iii) analysis of the stoichiometry of the layers. It is realized by electron energy loss spectroscopy (EELS) which is very sensitive to the thickness. Material has meanwhile to keep representative,

i.e. not too much amorphization, no contamination during the ion-milling, etc. . .<sup>4</sup>

Fig. 6 is a low magnification micrograph obtained in TEM bright field mode. Contrast is homogeneous on large zone (few tens of micrometer). The protocol meets the first requirement. It is asked to access the morphology and the thickness of each layer deposited in the core of the perform.

The third issue concerns the stoichiometry of the glass forming layers. Here the optimum thickness means that electron energy loss spectroscopy has to be possible in each layer. Thickness can be estimated by EELS spectroscopy. The estimation of thickness is realized by recording the zero-loss peak and computing the  $t/\delta_p$  ratio, following Egerton<sup>11</sup> where  $t$  is the thickness of the sample and  $\delta_p$ , mean free path associated to the volume plasmons. In the case of spectrum of Fig. 7:  $t/\delta_p = 0.6$ . This is a good value:  $t/\delta_p < 1$ .

Electron energy loss spectroscopy could be managed on such samples. The limitation is the spatial resolution, due to the very thin layers. This way stoichiometry for the various  $\text{Si}_x\text{B}_y\text{C}_z$  layers can be measured. Fig. 7 gives an example of the spectrum recorded on one of the  $\text{Si}_x\text{B}_y\text{C}_z$  layer. Amorphisation and contamination are supposed to be negligible: it could be verified by EELS that the stoichiometry variations managed by the processing parameters are effectively detected by EELS. This technique is only semi-quantitative.

The totality of these layers can be observed around isolated fibers, in the vicinity of large pores. With a regular protocol, thinning was impossible. Without the previous filling of the large pores with a material hard enough to undergo a slow ion-milling, the complete sequence cannot be inspected. This is the role of alumina cement introduced after the epoxy mounting (Section 2.3 of the experimental procedure). Alumina was selected for its slow milling-rate, comparable to that of  $\text{Si}_x\text{B}_y\text{C}_z$ .

It was seen that the infiltrated sequence in the core is never as large as the one deposited on the surface. The control of the intra-bundle sequence is important because the self-healing capability of the matrix requires enough

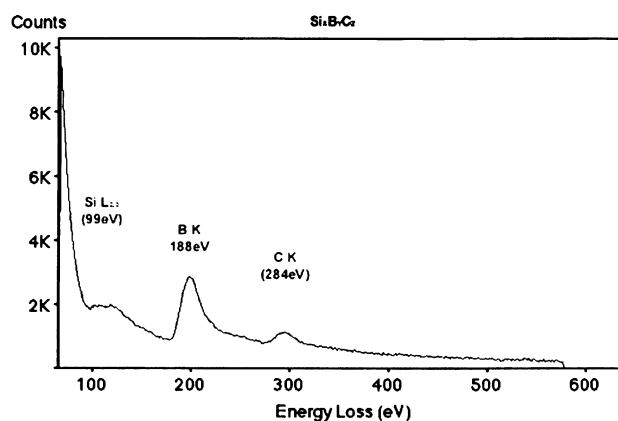


Fig. 7. Example of a EELS spectrum obtained on one of the  $\text{Si}_x\text{B}_y\text{C}_z$  layers of the matrix.

sublayers to be efficient. The completeness of the sequence observed near the large pores in the core, confirms that the chemical vapor infiltration mechanisms are well under control. The issue is the swelling of the dry bundle to open enough intra-bundle porosity and infiltrate an efficient sequence of matrix.

The second issue concerns the structure and the interface on the previous layer. Fig. 8 is a high resolution micrograph showing one of the first interfaces in-between the pyrocarbon and the SiC in the zone around the carbon fiber. Pyrocarbon presents a structure with a low density resulting from a weak anisotropy.<sup>8</sup> Silicon carbide growth occurs under the form of small crystals. High resolution shows that there is no transitory regime. The interface is well under control. Carbon fibers have a rough surface: the successive layers amplify the roughness. It is difficult to manage sharp interfaces as those obtained with silicon carbide reinforcement infiltrated by pulse-CVI.<sup>9</sup> On the CVI point of view, the requirement is met anyway: first in providing an optimal

fiber–matrix interfacing<sup>10</sup> and secondly in providing an efficient consolidation of the preform in the intra-bundle region.

#### 4. Conclusions

Additional mounting with alumina cement is the key point of this protocol. The thinning to electron transparency is double: first a mechanical thinning down to 20  $\mu\text{m}$  on a large surface with a tripod polisher then a final ion-milling (no dimpling). The sample is preferably cut in a test-specimen, after mounting in a very fluid epoxy bond. To optimize the infiltration of alumina cement, this step is done on 600  $\mu\text{m}$ -thick slices. For an efficient observation of the mechanical parameters the longitudinal fibers in the TEM sample have to be the 0°-bundle of the tensile test specimen.

The protocol describes seven different steps: (i) sectioning, (ii) slice selection, (iii) mounting, (iv) polishing the

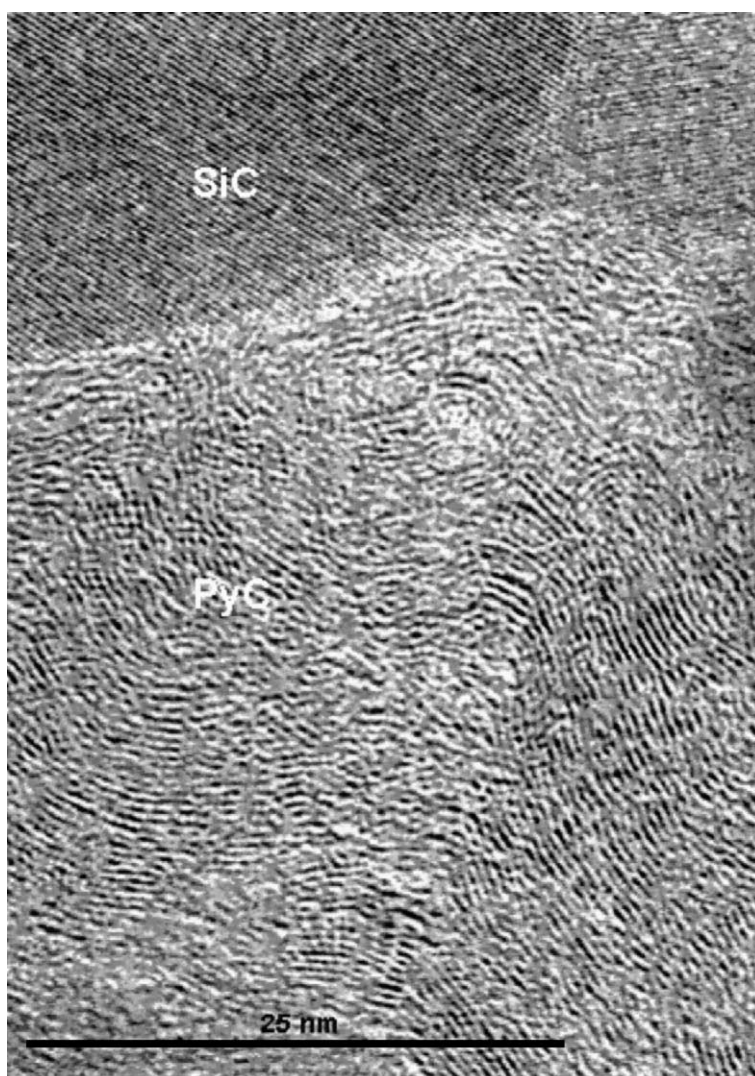


Fig. 8. Structure in high resolution TEM mode of one of the carbon/SiC interface around the fiber.

face of interest, (v) drilling and sticking the specimen on the TEM copper grid, (vi) mechanical thinning (strictly speaking) and polishing of the second face down to 20  $\mu\text{m}$ , and finally (vii) the ion-beam milling to get the final thickness.

High resolution TEM can be performed as well as EELS spectroscopy proving the efficiency of the technique.

### Acknowledgements

Authors wish to thank Francois Doux, TEM microscopist from Snecma Propulsion Solid as well as Michel Bourgeon for their help in this work. AM wish to thank CNRS and SPS for granting here thesis.

### Appendix A. Mounting in alumina cement

Alumina cement 503 from Aremco is distributed by TTA in Europe. Its residual porosity is given to be less than 1% after curing. It has a good resistance to acetone and ethanol. This product is sensitive to water after curing or basic finishing lubricant, thus water-free lubricant are necessary. Also this cement contains 1–3% of phosphoric acid (possible artifacts). Few droplets of cement are poured on a glass slide. The thick foil is put on it and the cement is forced through it, gently. The same operation is done on the other side. At the end, the slice is covered again with cement and put 2 min in the embedding chamber in vacuum (10 kPa). Afterward the excess of cement is eliminated, the slice is dried few hours at room temperature, then 60 °C for the night on a silicone gum pad. Finally the cement is cured following the supplier heating ramp.

### References

1. Jacques, S., Guette, A., Langlais, F. and Bourrat, X., Characterization of SiC/C(B)/SiC microcomposites by transmission electron microscopy. *J. Mater. Sci.* 1995, **32**, 381–388.
2. Naslain, R., Bourrat, X., Pailler, R. and Lamon, J., Mimicking the layered structure of natural shells as a design approach to the fiber–matrix interfaces. In *Proceedings of ECCM-8, Naples June 3–6, 1998, Vol 4*, ed. I. Crivelli-Visconti. Woodhead Publ. Ltd., Cambridge, UK, 1998, pp. 191–199.
3. Bertrand, S., Droillard, C., Pailler, R., Bourrat, X. and Naslain, R., 2D SiC/SiC CVI-composites with a (C–SiC)<sub>n</sub> multilayer interphase: processing, microstructure and tensile behavior at 25 °C. *J. Eur. Ceram. Soc.* 2000, **20**, 1–13.
4. Goodhew, P. J., Thin foil preparation for electron microscopy. In *Practical Methods in Electron Microscopy, Vol 11*, ed. A. M. Glauret. Elsevier, 1985.
5. Klepeis, S. J., Benedict, J. P. and Anderson, R. M., A grinding/polishing tool for TEM sample preparation. *MRS Symp. Proc.* 1988, **115**, 179–184.
6. Ayache, J. and Albarede, P. H., Application of the ionless tripod polisher to the preparation of YBCO superconducting multilayer and bulk ceramics thin films. *Ultramicroscopy* 1995, **60**, 195–206.
7. Buseck, P. R., Cowley, J. M. and Eyring, L., *High-Resolution Transmission Electron Microscopy*. Oxford University Press, New York, Oxford, 1988.
8. Bourrat, X., Trouvat, B., Limousin, G., Vignoles, G. L. and Doux, F., Pyrocarbon anisotropy as measured by electron diffraction and polarised light. *J. Mater. Res.* 2000, **15**, 92–101.
9. Naslain, R., Pailler, R., Bourrat, X. and Vignoles, G. L., Processing of ceramics matrix, composites by pulse-CVI and related techniques. In *Proceedings of the International Symposium on Novel Synthesis and Processing of Ceramics, Kurume, Fukuoka, October 26–29, 1997*; Key Eng. Mater. 1999, **159/160**, 359–366.
10. Droillard, C., Lamon, J. and Bourrat, X., Strong interfaces in CMCs: the condition for efficient multilayered interfaces. *Mater. Res. Soc. Symp. Proc.* 1995, **365**, 371–376.
11. Egerton, R. F., *Electron Energy-Loss Spectroscopy in the Electron Microscope*. Plenum Press, New York, London, 1986, ISBN 0-306-42158-5.